ISME

Free and Forced Vibration Behavior of Cylinders Made of Two Dimensional Functionally Graded Materials using Meshless Method

H. Mirzaei[*]
M.Sc.

S.A.S. Roknizadeh[†]
Assistant Professor

In this article, a meshless method is developed to analyze free and forced vibration behavior of axisymmetric cylinders made of two dimensional functionally graded materials (2D-FGMs). The meshless method is the based on weak form of motion equations using the moving least square (MLS) shape functions. The 2D-FGM cylinders are made of a mixture of a ceramic and a metal. The volume fraction of each component is assumed to be functionally varied along both radial and axial directions of cylinders. The effects of profile of material distributions, cylinder dimensions, boundary conditions and loading on the vibrational characteristics of the proposed 2D-FGM cylinders are investigated. The results of investigating the vibrations of the cylinders made of 2D-FGM confirmed that in the engineering design applications, the radial vibrations can be attenuated by adjusting the power coefficients along the radius and length of the cylinder.

DOI: 10.30506/jmee.2020.117657.1210

Keywords: Free and forced vibrations, meshless method, functionally graded materials.

1 Introduction

The uniform gradient of material properties in the functionally graded material (FGM) reduces the stress concentration at interfaces while improving the strength of the bond between two different materials, and hence enhances the resultant mechanical characteristics. The FGMs can be used for producing heat shields in the aerospace industry, turbine blades, and cutting components, among other applications in many other industries including the nuclear, energy, automotive, and medicine industries. Given the crucial importance of such components shelf life in various industries, it should be viable to measure and reduce the vibration of such equipment to the extent possible so as to ascertain production of longer lasting parts.
Accordingly, in the present paper, FGMs are modeled two-dimensionally to measure vibrations and achieve the mentioned objectives. In recent years, numerous research works have been performed on the vibrational and dynamic behavior of FGM-made and multi-layer cylinders. Loy and Lam [1] used the Love's first-approximation theory and Ritz method to investigate the effect of volumetric fraction constant and boundary conditions on the natural frequencies of the FGM-made cylinders.

[*] M.Sc., Department of Mechanical Engineering, Ahvaz Branch, Islamic Azad University, Ahvaz, Iran
Habib.mirzaie85@gmail.com
[†] Corresponding Author, Assistant Professor, Department of Mechanical Engineering, Ahvaz Branch, Islamic Azad University, Ahvaz, Iran ali_roknizadeh@yahoo.com
Receive : 2019/11/28 Accepted : 2020/07/24

In a similar piece of research, Pradhan and Lam [2] used the Love's theory to analyze the vibrations of a cylindrical FGM-made shell under different support conditions, where they investigated the relationship between the obtained natural frequencies and the considered material properties. In this work, the material properties were graded along the thickness of the shell according to a power function. On the other hand, Zhou and Chung [3] presented an analysis on 3D vibrations of hallow and solid cylinders through the Chebyshev-Ritz method. Their analysis was based on the small-strain, linear, and exact elasticity theories. Hadadpoor and Mahmoodkhani [4] further examined free vibrations of simply supported FGM-made cylindrical shells under four sets of planar boundary conditions. They considered temperature-dependent material properties that varied along the shell thickness and used the Galerkin method to solve the formulated problem. Najafizadeh [5] investigated free vibrations of an FGM-made ring-reinforced cylindrical shell based on the high-order theory. Natural frequencies were calculated using the Rayleigh–Ritz method. This paper showed that the position of the ring imposes a significant impact on the fundamental frequency, and that the impact changes with changes in the volumetric fraction. For a simply supported FGM-made cylindrical shell, the fundamental frequency is maximal when the ring is situated in the middle of the shell. The dominant frequency decreases as the ring gets farther from the middle of the shell. This implies the symmetrical nature of the curve of fundamental frequency around the center of the shell. Ansari and Darvizeh [6] investigated free vibrations of an FGM-made shell under a variety of boundary conditions analytically (exact solution). Their theories were based on the first-order shear deformation theory for the shells, where radial variations of the material properties were assumed to be a power function of temperature. In this work, the effects of volumetric fraction power and possible changes in geometrical parameters on the vibrational characteristics were ignored. Given the advantages offered by meshless methods, as compared to finite-element methods, such as the elimination of the meshing stage and insensitivity to the network balance, such methods have been increasingly applied in recent years. Molarazi et al. [7] investigated the 1D free vibrations of an FGM-made cylinder using a meshless method called moving least squares (MLS). They utilized the weak form of the equation and a weighting function to calculate the shape function. Forootan et al. [8] computed one-dimensional free vibrations of an FGM-made cylinder using n meshless method called Hermitian function.

Being different from the weak-form meshless methodologies, this method required neither cellular meshing nor numerical integration. The elimination of the numerical integration stage addressed such limitations as the time-intensiveness and poor accuracy of the solution, and the equations could be directly determined using the strong form of the governing partial differential equations. The main problem with this methodology was the instability of the solution, especially when the boundary conditions involved derivatives. Here the derivative-involving boundary conditions were applied through Hermitian shape functions and hence enhanced the solution accuracy significantly. Sadeghi and Sohrabi [9] presented dynamic analysis of an FGM-made cylinder under loading using the meshless local Petrov-Galerkin (MPLG) method. Basically, the method was based on the weak local form and principles of interpolation. Safaei et al. [10] calculated the forced vibration frequencies of an FGM-made cylinder under thermomechanical loading using a meshless procedure. They considered the effect of the loading frequency on the dynamic behavior of the nanocomposite sandwich panels under thermomechanical loading scenarios, where the studied structures were exposed to not only periodic mechanical loading, but also thermal gradients. The polymer matrix material properties were assumed to be temperature-dependent, and a high-order shear deformation theory-based meshless method was used to achieve accurate results. The authors further examined the impacts of the mechanical loading frequency, the thermal gradient load, and the boundary conditions on the forced vibrations and the resonance, observing that the thermal gradient loads imposed a significant impact on the amplitude of the vibrations of the

nanocomposite sandwich panels. In the following, we present examples of studies where dynamic analysis of FGM-made cylinders was done using meshless techniques. As indicated by many studies, most of the research works have considered the FGM one-dimensionally, i.e. graded along the thickness only.

Based on the core idea that the vibrations of an FGM-made cylinder can be controlled by restructuring the cylinder configuration, the present paper considers a graded cylinder not only along the radius, but also along its length. This basis is then used to reconstruct the governing equations for this new structure to come with a new set of governing equations. Continuing with the work, the location vector is approximated using MLS approximation, a meshless method, and the weak form of the equation of motion, with the spline weighting function used to obtain the shape function. Next, the value of strain is calculated using the displacement vector before computing the mass and stiffness matrices, by which one can formulate an Eigen value problem for the free vibrations. Accordingly, the forced vibrations can be calculated by applying a force to the system.

2 The governing equations

In the present work, the FGM-made cylinder demonstrated in Figure (1) is considered. The FGM is composed of ceramic and steel.

The material properties are assumed to change uniformly and continuously along both thickness and length of the cylinder based on the modified power model, as follows:

$$P(r,z) = (P_o - P_i)\left(\frac{r-r_i}{r_o-r_i}\right)^n \left(\frac{z}{L_z}\right)^m + P_i \tag{1}$$

Where p denotes the constituent material property (e.g. Young's modulus, density, and Poisson's ratio). For the present problem, P_i and P_o denote the properties of the inner and outer layers of the cylinder, respectively.

Given the above equation, 2D volumetric variations of the FGM-made cylinder could be calculated from Eq. (2):

$$V_f = \left(\frac{r-r_i}{r_o-r_i}\right)^n * (\frac{z}{L_z})^m \tag{2}$$

Where V_f is the volumetric fraction of the material, and m and n are positive constants. This equation is made up of two parts. The first part describes the volumetric fractions along the radius while the second part expresses the variations along the length of the cylinder.

If m = 0, then the volumetric variations will be considered one-dimensionally, i.e. along the radius of the cylinder only, while n = 0 implies that the volumetric variations occur one-dimensionally along the cylinder length only. Figure (2) shows the volumetric variations for the case where m = 2 and n = 1, from the inner silicon carbide layer to the outer stainless-steel layer.

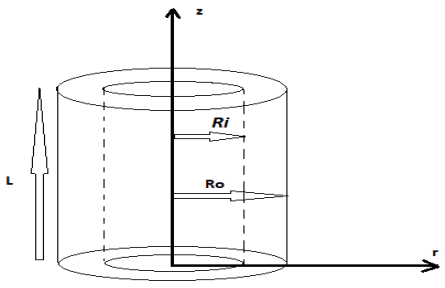

Figure1 Axisymmetric cylinder

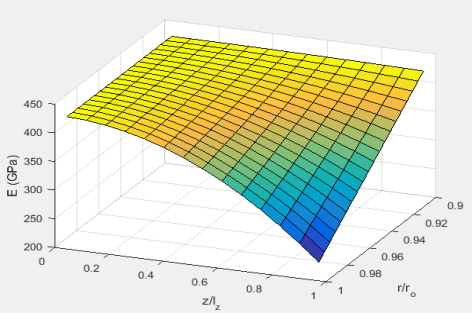

Figure 2 Radial vibrations with an outer radius of 0.2 and an inner radius of 0.18 under three different uploading at m=2, n=10

In terms of the boundary conditions, the cylinder is assumed to be fixed along its axis at both ends. This assumption smooths the way toward solving the problem two-dimensionally rather than three-dimensionally, i.e. considering an axially symmetric cylinder.

3 Weak form of the equation of motion

According to the virtual work principle, the weak form of the equation of motion in absence of external forces is as follows [7]:

$$\int_{\Omega} \boldsymbol{\sigma}\delta(\boldsymbol{\varepsilon})\,dv - \int_{\Gamma} \mathbf{F}\delta\mathbf{u}\,ds + \int_{\Omega} \rho(r)\,\delta\mathbf{u}\ddot{\mathbf{u}}\,dv = 0 \tag{3}$$

$$\begin{aligned}
\sigma_r &= \frac{E}{1-\nu^2}(\varepsilon_r + \nu\varepsilon_\theta + \nu\varepsilon_z)\\
\sigma_\theta &= \frac{E}{1-\nu^2}(\varepsilon_\theta + \nu\varepsilon_r + \nu\varepsilon_z)\\
\sigma_z &= \frac{E}{1-\nu^2}(\varepsilon_z + \nu\varepsilon_r + \nu\varepsilon_\theta)\\
\sigma_{rz} &= G\gamma_{rz}
\end{aligned} \tag{4}$$

Where σ, ε, F, and U denote the vectors of stress, strain, surface force, and displacement, respectively. Γ is a segment of the region Ω on which the surface force, F, is applied. The stress-strain equation for an axially symmetric body in the cylindrical coordinate system is as follows and the above-mentioned equations can be expressed in matrix form, as follows:

$$\sigma = S\,\varepsilon \tag{5}$$

$$\mathbf{S} = \frac{E}{(1+\nu)(1-2\nu)}\begin{bmatrix} 1-\nu & \nu & \nu & 0 \\ \nu & 1-\nu & \nu & 0 \\ \nu & \nu & 1-\nu & 0 \\ 0 & 0 & 0 & \frac{(1-2\nu)}{2} \end{bmatrix} \quad ,E = E(r,z)\ ,\nu = \nu(r,z)$$

Onateh et al. [11] proved that the MLS approximation can be used to obtain approximation of a particular function in a meshless fashion in such a way to minimize the sum of squares (SSQ)

at each node based on the weight or the impact of each node on the approximation. Then, the Jacobi function takes the following form:

$$J = \sum_{i=1}^{N} w(u^h(\mathbf{X}_i) - u(\mathbf{X}_i))^2 = \sum_{i=1}^{N} w(\mathbf{P}^{\mathrm{T}}(\mathbf{X}_i)\mathbf{a} - u_i)^2 \tag{6}$$

In the standard least squares (LSQ) method, in order to minimize the SSQ of the Eq. (6), its derivative with respect to the unknown coefficients vector, a, is set to zero.

$$\frac{\partial J_{\overline{\mathrm{X}}}(\mathbf{a})}{\partial \mathbf{a}} = 0 \Rightarrow \sum_{i=1}^{N} w(\overline{\mathbf{X}} - \mathbf{X}_i) 2\mathbf{P}(\mathbf{X}_i)[\mathbf{P}^{\mathrm{T}}(\mathbf{X}_i)\mathbf{a}(\overline{\mathbf{X}}) - u_i] = 0$$

$$2\sum_{i=1}^{N} w(\overline{\mathbf{X}} - \mathbf{X}_i)\mathbf{P}(\mathbf{X}_i)\mathbf{P}^{\mathrm{T}}(\mathbf{X}_i)\mathbf{a}(\overline{\mathbf{X}}) - w(\overline{\mathbf{X}} - \mathbf{X}_i)\mathbf{P}(\mathbf{X}_i)u_i] = 0. \tag{7}$$

$$\sum_{i=1}^{N} w(\overline{\mathbf{X}} - \mathbf{X}_i)\mathbf{P}(\mathbf{X}_i)\mathbf{P}^{\mathrm{T}}(\mathbf{X}_i)\mathbf{a}(\overline{\mathbf{X}}) = w(\overline{\mathbf{X}} - \mathbf{X}_i)\mathbf{P}(\mathbf{X}_i)u_i. \tag{8}$$

In the above equations, a ($\bar{X}$) is the unknown coefficients vector, including the central fixed point $\bar{X}$, and P(X) is the complete basis vector. in the meshless method used in this research, the MLS shape functions were used, and the components of the displacement vector were approximated at each point, as follows:

$$u^h(\mathbf{X}) = \mathbf{P}^{\mathrm{T}}(\mathbf{X})\left[\sum_{i=1}^{N} w(\overline{\mathbf{X}} - \mathbf{X}_i)\mathbf{P}(\mathbf{X}_i)\mathbf{P}^{\mathrm{T}}(\mathbf{X}_i)\right]^{-1}\sum_{i=1}^{N} w(\overline{\mathbf{X}} - \mathbf{X}_i)\mathbf{P}(\mathbf{X}_i)u_i. \tag{9}$$

Where W is the weighting function and uh(x) is the real component of the displacement in x direction of the cylindrical coordinate system. Here we utilized the spline weighting functions with a 2D (rectangular) weighting function obtained from the following tensor product:

$$(\boldsymbol{x} - \boldsymbol{x_i}) = w\left(\frac{r - r_i}{\rho_r}\right) w\left(\frac{z - z_i}{\rho_z}\right), \quad \rho_r = d_{max}, \Delta\bar{r} \quad , \quad \rho_z = d_{max}, \Delta\bar{z} \tag{10}$$

Ultimately, Eq. (11) represent the final function:

$$u^h(x) = \sum_{I=1}^{NP} \Psi_I(x) u_I \tag{11}$$

Where NP represents the number of nodes within the affected region, Ψ_I (x) is the meshless MLS shape function, u_i is the generalized (virtual) displacement of the nodes within the affected region around the considered point, and uh is the actual displacement of the point. Under axial symmetry, each point in the cylindrical coordinate system has two displacement components that can be approximated using Eq. (12).

$$u_r^h(x) = \sum_{i=1}^{NP} \Psi_i(u_r)_i$$

$$u_z^h(x) = \sum_{i=1}^{NP} \Psi_i(u_z)_i \tag{12}$$

In the above equation, Ψ_i is the shape function of the i-th node, $(u_r)_i$ and $(u_z)_i$ are components of the generalized displacement at the respective nodes, u_r^h is the actual displacement component along r-axis, and u_z^h is the actual displacement component along z-axis of the cylindrical coordinate system. The following equation gives the strain as a function of displacement:

$$\boldsymbol{\varepsilon} = \mathrm{Q}\mathbf{u} \tag{13}$$

$$\mathbf{u} = \left[(u_r)_1, (u_z)_1, \ldots\ldots\ldots (u_r)_N, (u_z)_N\right]^T \tag{14}$$

$$\mathrm{Q} = \begin{bmatrix} \frac{\partial \Psi_1}{\partial r} & 0 & \frac{\partial \Psi_2}{\partial r} & 0 & \ldots & \frac{\partial \Psi_N}{\partial r} & 0 \\ \frac{\Psi_1}{r} & 0 & \frac{\Psi_2}{r} & 0 & \ldots & \frac{\Psi_N}{r} & 0 \\ 0 & \frac{\partial \Psi_1}{\partial z} & 0 & \frac{\partial \Psi_2}{\partial z} & \ldots & 0 & \frac{\partial \Psi_N}{\partial z} \\ \frac{\partial \Psi_1}{\partial z} & \frac{\partial \Psi_1}{\partial r} & \frac{\partial \Psi_2}{\partial z} & \frac{\partial \Psi_2}{\partial r} & \ldots & \frac{\partial \Psi_N}{\partial z} & \frac{\partial \Psi_N}{\partial r} \end{bmatrix} \tag{15}$$

The weak form of the equation for free vibrations (i.e. under zero driving force) is obtained as follows:

$$\left(\int_\alpha \rho(r.z)\Psi^T\Psi dv\right)\ddot{u} + \left(\int_\alpha Q^T S Q\, dv\right)u = 0 \tag{16}$$

Eq. (16) is a function of acceleration and displacement vectors wherein the mass and stiffness matrices are calculated through Eqs. (17) - (18), respectively.

$$M = \int_\alpha \rho(r.z)\Psi^T\Psi dv \tag{17}$$

$$K = \int_\alpha Q^T S Q\, dv \tag{18}$$

Substituting Eqs. (17) - (18) into Eq. (16) gives Eq. (19):

$$\hat{\mathbf{M}}\ddot{\mathbf{U}} + \hat{\mathbf{k}}\mathbf{U} = 0 \tag{19}$$

Eq. (19) can be solved by solving the Eigen value problem formulated in Eq. (2):

$$\left|\mathrm{d} - \mathrm{I}\,\lambda_i\right| = 0 \tag{20}$$

Where $\mathbf{d} = \mathbf{M}^{-1} \times \mathbf{k}$ and $\lambda_i = \omega_i^2$.

4 Validation

Firstly, an FGM-made cylinder with an inner layer of silicon carbide and an external layer of stainless steel was considered. Mechanical properties of the two materials are presented in Table (1). Table (2) lists the first 8 natural frequencies of the solid and hollow cylinders at length-to-outer radius ratios of $L / r_o = 3$ and 6 and inner-to-outer radius ratios of $r_i / r_o = 0$ and 0.5 when the cylinder is fixed at both ends. As observed, the accuracy of the meshless method was more than enough for both hallow and solid cylinders, as indicated by the good agreement with the results presented in the respective reference. Moreover, the results imply that the solid cylinders exhibit higher values of natural frequency compared to the respective hallow cylinders when their length is equal to their outer radius.

5 Results of free vibrations of cylinder made of 2D-FGM

Regarding the boundary conditions, the cylinder was assumed to be pinned at both ends. Inner radius, outer radius, and height of the cylinder were set to 0.18, 0.2, and 1, respectively.
In Table (3), as mentioned earlier, the case with m = 0 represents a 1D model of the cylinder along its radius. By changing the values of the coefficients m and n, changes were observed in the natural frequency of the system and the concentration of ceramic in the steel; that is, an increase in m increased the natural frequency of the system, and hence lowerd the chances of resonance phenomenon.

Table 1 mechanical properties of FGM components[7]

materials	E(N/m^2)	ν	ρ(kg/m^3)
Silicon carbide (SiC)	427×10^9	0.17	3210
Stainless steel (SUS304)	207.78×10^9	0.3177	8166

Table 2 The first 8 natural frequencies for axially symmetric vibrations of homogeneous solid/hallow pinned-non-pinned cylinders and comparison with Ref. [3] for different length-to-outer radius ratios.

L/r_o	ri/ro	Method	Ω_1	Ω_2	Ω_3	Ω_4	Ω_5	Ω_6	Ω_7	Ω_8
3	ri/ro =0	Meshless	1.7219	3.0723	3.5368	4.0556	4.0969	4.1841	4.8423	5.059
3	ri/ro = 0	[3]	1.7159	3.062	3.5339	4.0485	4.0849	4.1789	4.8245	5.0181
3	ri/ro=0.5	Meshless	1.7004	2.3135	2.5657	2.8981	3.6206	3.6642	4.4991	5.2965
3	ri/ro=0.5	[3]	1.6949	2.3123	2.5607	2.8798	3.5883	3.6514	4.4161	5.2166
6	ri/ro =0	Meshless	0.8569	1.6822	2.4108	2.9334	3.3019	3.54962	3.676	3.7678
6	ri/ro = 0	[3]	0.8543	1.6758	2.3982	2.919	3.2745	3.5289	3.6712	3.7271
6	ri/ro=0/5	Meshless	0.854	1.651	2.1278	2.2901	2.4044	2.4063	2.6044	2.7638
6	ri/ro=0.5	[3]	0.8508	1.6432	2.1214	2.2847	2.3954	2.4041	2.5794	2.7288

Based on the values reported in Table (3), it can be observed that the more rigid the body (i.e. the higher the concentration of the silicon carbide compared to the steel), the higher would be the values of natural frequency. These different variations for the FGM-made cylinders were attributed to the inverse behavior of the density with respect to the modulus of elasticity or Poisson's ratio, and also the fact that the effect of density dominates those of the modulus of elasticity or Poisson's ratio at lower powers. According to Eq. (2), the coefficients m and n were used to impose changes along the radius and length of the FGM-made.

As is shown in Table (3), a decrease in the value of m from 2 to 0.5 lowered the resultant natural frequencies. That is, higher natural frequencies were obtained with increasing the ceramic concentration (i.e. stiffness of cylinder material), and vise verse.
In a next stage, effects of different power coefficients on the natural frequencies were investigated two-dimensionally by decreasing the inner radius of the cylinder, with the results presented in Table (4).

Based on the obtained values of natural frequency, it was evident that a decrease in the thickness lowered the natural frequency of the system, and that in a two-dimensional domain, one can control the rate of natural frequency drop by adjusting the power coefficients; this latter finding offers evolutionary advantages for the engineering design of engineering and aerospace equipment. As we know, the stiffness and mass matrices are the most important factors affecting the natural frequency of a body. Accordingly, the lower the mass, the higher is the natural frequency. This implies that higher natural frequencies may be expected upon increasing the thickness.

Table 3 Comparison of the first five frequencies between 1D and 2D cylinders with different power coefficients and the following specifications: $L / r_o = 5$, $L_z = 1$, $r_i / r_o = 0.9$, $r_o = 0.2$, and $r_i = 0.18$).

Ω	FGM cylinder	Material	Coefficients	n = 1	n = 5	n = 10	Material
Ω_1	1D	SUS304	m = 0	0.648597	0.666583	0.689423	Sic
Ω_1	2D	SUS304	m = 0.5	0.69977	0.85617	0.90082	Sic
Ω_1	2D	SUS304	m = 2	0.81346	0.90857	0.93171	Sic
Ω_2	1D	SUS304	m = 0	0.885265	0.911222	0.944183	Sic
Ω_2	2D	SUS304	m = 0.5	1.09581	1.3838	1.46393	Sic
Ω_2	2D	SUS304	m = 2	1.20262	1.44613	1.50627	Sic
Ω_3	1D	SUS304	m = 0	1.10747	1.137963	1.176599	Sic
Ω_3	2D	SUS304	m = 0.5	1.12097	1.40686	1.48477	Sic
Ω_3	2D	SUS304	m = 2	1.27734	1.48338	1.53394	Sic
Ω_4	1D	SUS304	m = 0	1.135263	1.166363	1.205777	Sic
Ω_4	2D	SUS304	m = 0.5	1.16443	1.43249	1.50881	Sic
Ω_4	2D	SUS304	m = 2	1.3717	1.52287	1.55842	Sic
Ω_5	1D	SUS304	m = 0	1.16271	1.194439	1.234659	Sic
Ω_5	2D	SUS304	m = 0.5	1.20718	1.4543	1.52441	Sic
Ω_5	2D	SUS304	m = 2	1.44457	1.55047	1.5766	Sic

Table 4 Comparison of the first five frequencies with decreasing the thickness and changing the power coefficients on cylinders of the following specifications: $L / r_o = 5$, $L_z = 1$, and $r_o = 0.2$).

Ω	Material	ro= 0.20	n = 1, m = 0.5	n = 5, m = 0.5	n = 10, m = 0.5	Material
Ω1	SUS304	ri = 0.18	0.69977	0.85617	0.90082	Sic
Ω1	SUS304	ri = 0.16	0.69999	0.85910	0.90179	Sic
Ω1	SUS304	ri = 0.14	0/70173	0.86061	0.90582	Sic
Ω2	SUS304	ri = 0.18	1.09581	1.38380	1.46393	Sic
Ω2	SUS304	ri = 0.16	1.19516	1.48373	1.56185	Sic
Ω2	SUS304	ri = 0.14	1.27077	1.56962	1.65106	Sic
Ω3	SUS304	ri = 0.18	1.12097	1.40686	1.48477	Sic
Ω3	SUS304	ri = 0.16	1.20145	1.50635	1.59420	Sic
Ω3	SUS304	ri = 0.14	1.29153	1.61184	1.70410	Sic
Ω4	SUS304	ri = 0.18	1.16443	1.43249	1.50881	Sic
Ω4	SUS304	ri = 0.16	1.29209	1.56118	1.63306	Sic
Ω4	SUS304	ri = 0.14	1.41356	1.68606	1.75857	Sic
Ω5	SUS304	ri = 0.18	1.20718	1.45430	1.52441	Sic
Ω5	SUS304	ri = 0.16	1.37957	1.62435	1.69315	Sic
Ω5	SUS304	ri = 0.14	1.49358	1.79509	1.88327	Sic

Now, let us consider the effects of the cylinder length and variations of the power coefficients on the natural frequencies.

Table 5 Comparison of the first five frequencies with decreasing the cylinder length and changing the power coefficients on cylinders of the following specifications: $r_i / r_o = 0.9$, $r_o = 0.2$, and $r_i = 0.18$).

Ω	Material	L	n = 1, m = 0.5	n = 5, m = 0.5	n = 10, m = 0.5	Material
Ω1	SUS304	L=1	0.6967	0.8526	0.8996	Sic
Ω1	SUS304	L=0.4	1.1815	1.4619	1.5396	Sic
Ω1	SUS304	L=0.2	1.3853	1.6781	1.7624	Sic
Ω2	SUS304	L=1	1.2708	1.5696	1.6511	Sic
Ω2	SUS304	L=0.4	1.2838	1.5452	1.6184	Sic
Ω2	SUS304	L=0.2	2.1974	2.6403	2.7721	Sic
Ω3	SUS304	L=1	1.2915	1.6118	1.7041	Sic
Ω3	SUS304	L=0.4	1.5576	1.8625	1.9516	Sic
Ω3	SUS304	L=0.2	3.6055	4.3721	4.5978	Sic
Ω4	SUS304	L=1	1.4136	1.6861	1.7586	Sic
Ω4	SUS304	L=0.4	1.8099	2.1916	2.3028	Sic
Ω4	SUS304	L=0.2	3.6561	4.3948	4.6166	Sic
Ω5	SUS304	L=1	1.4936	1.7951	1.8833	Sic
Ω5	SUS304	L=0.4	2.0718	2.472	2.593	Sic
Ω5	SUS304	L=0.2	5.5575	6.6982	7.0402	Sic

The results presented in Table (5) indicate that, for the cylinder made of 2D-FGM, a decrease in the cylinder length and/or an increase in the power coefficients, n, enhances the natural frequency. This finding provides great help for the design of engineering equipment. Indeed, one can increase the value of n by enhancing the concentration of ceramic, which leads to improved stiffness of the system and hence retards the resonance phenomenon.

6 Investigation of forced vibrations in cylinders made of 2D-FGM

In this subsection, harmonic forced vibrations of cylinders made of 2D- FGM are investigated. For this purpose, the loading scheme was considered as mentioned in Eq. (21).

$$p_i = 10\ sin\ (\frac{5\pi}{0{,}0015}t) \tag{21}$$

Here the force is assumed to be internally applied to the cylinder made of FGM, i.e. the cylinder undergoes periodic loading and unloading of the force. Now, the dimensional and loading variations across the cylinder made of 2D-FGM were as follows.

In Figures (3) and (4), radial vibrations are investigated for an outer radius of 0.2 and an inner radius of 0.18 under three different stimulation frequencies for different values of m and n.

In both figures, n = 10, with the value of m being set to 2 and 0.5 for Figures (3) and (4), respectively. Carefully comparing the radial vibrations between Figures (3) and (4), it is evident that a decrease in the value of m (i.e. decreasing the cylinder material stiffness) from 2 to 0.5 attenuated the radial vibrations.

In fact, one could attenuate the radial vibrations of the cylinder by making the cylinder functionally graded in two dimensions and modifying the equations describing the volumetric fraction variations. This has been a primary objective of the present research: attenuation of radial vibrations. Figures (5)–(7) demonstrate the vibrations of an FGM-made cylinder with an outer radius of 0.2 and an inner radius of 0.18 under periodic loading at 100 kHz for different values of m and n.

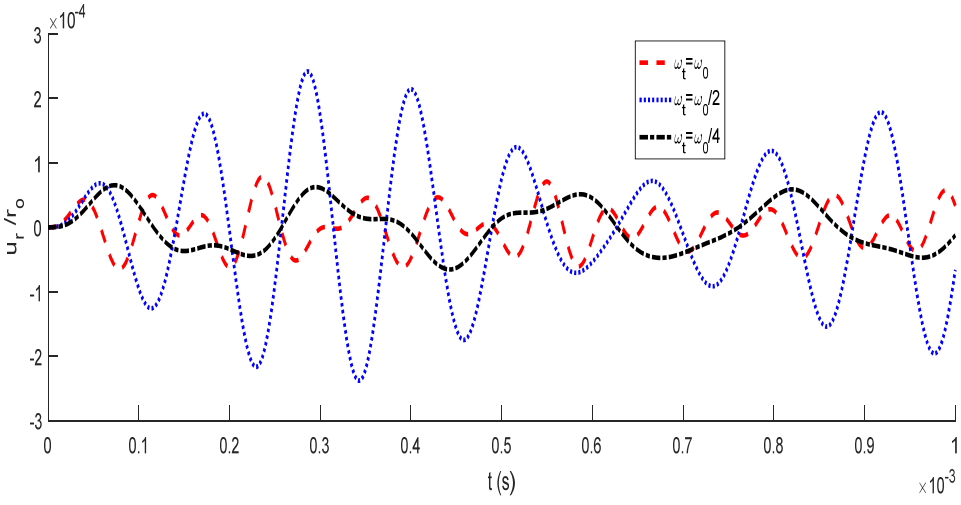

Figure 3 Radial vibrations of a cylinder with an outer radius of 0.2 and an inner radius of 0.18 under three loading schemes with m = 2 and n = 10.

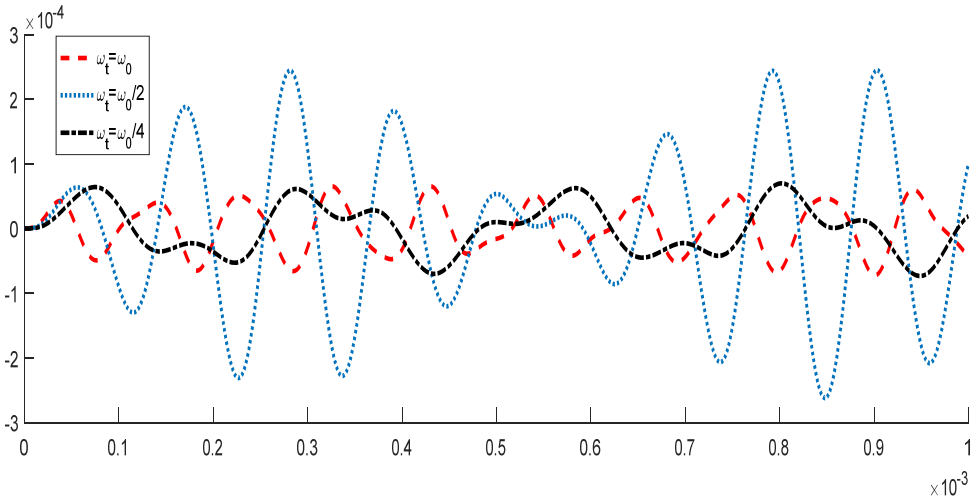

Figure 4 Radial vibrations of a cylinder with an outer radius of 0.2 and an inner radius of 0.18 under three loading schemes with m = 0.5 and n = 10.

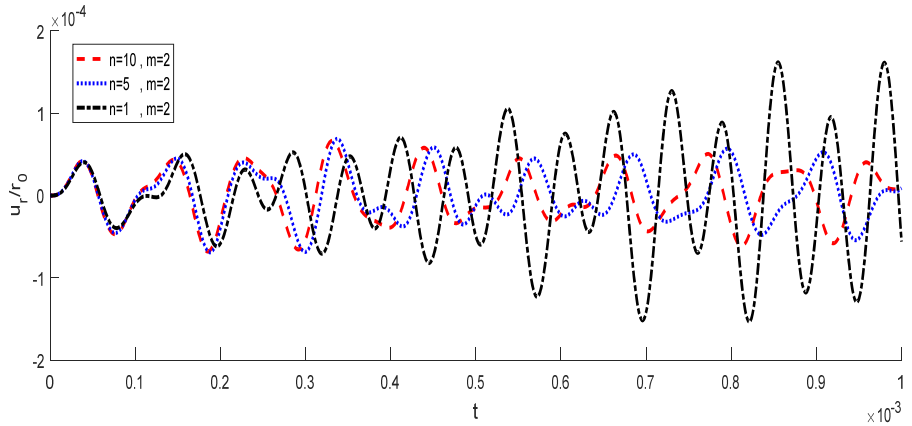

Figure 5 Radial vibrations of a cylinder with an outer radius of 0.2 and an inner radius of 0.18 with constant m and varying n.

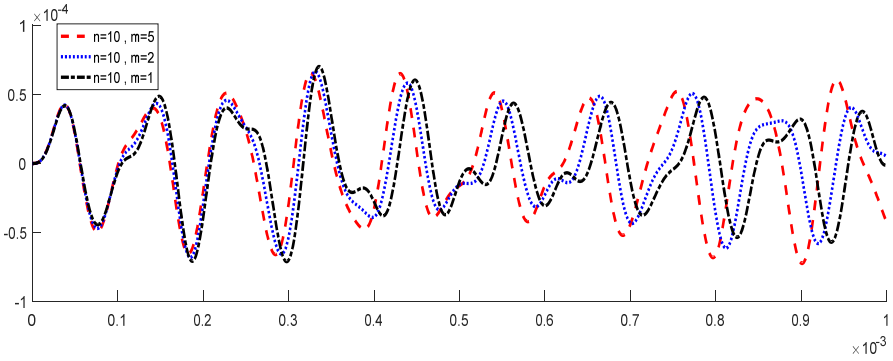

Figure 6 Radial vibrations of a cylinder with an outer radius of 0.2 and an inner radius of 0.18 with constant m and varying n.

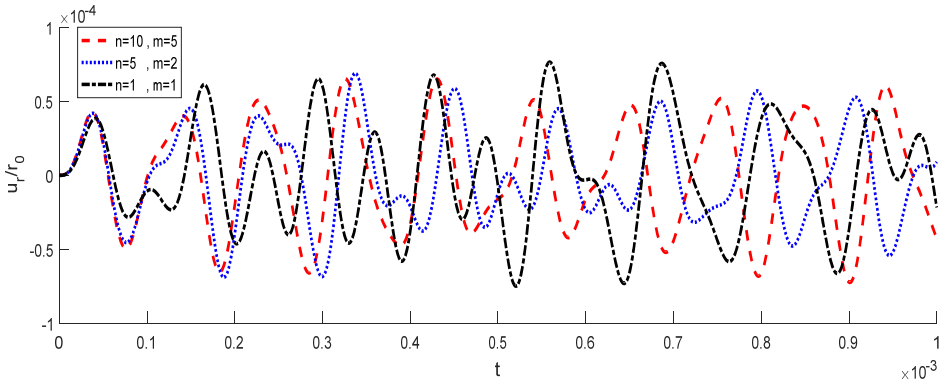

Figure 7 Radial vibrations of a cylinder with an outer radius of 0.2 and an inner radius of 0.18 with varying both m,n.

Now, decreasing the inner radius of the cylinder to 0.16 (thereby increasing the cylinder thickness), the vibrations were recalculated for the three cases.

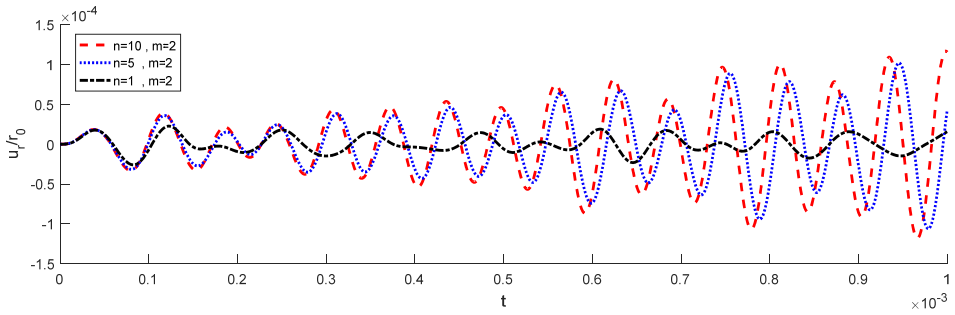

Figure 8 Radial vibrations of a cylinder with an outer radius of 0.2 and an inner radius of 0.16 and height of 1 with constant m and varying n.

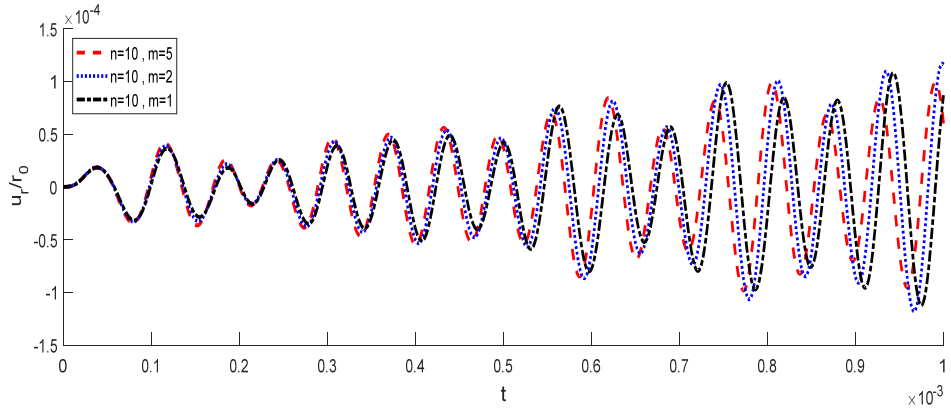

Figure 9 Radial vibrations of a cylinder with an outer radius of 0.2 and an inner radius of 0.16 and height of 1 with constant n and varying m.

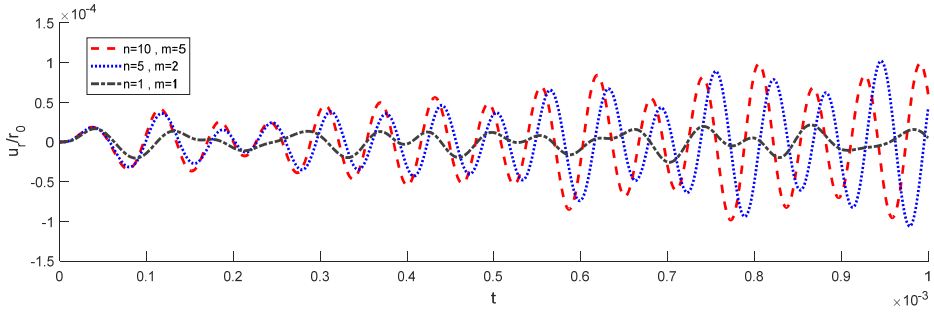

Figure 10 Radial vibrations of a cylinder with an outer radius of 0.2, inner radius of 0.16, and a length of 1 for different values of *m* and *n*.

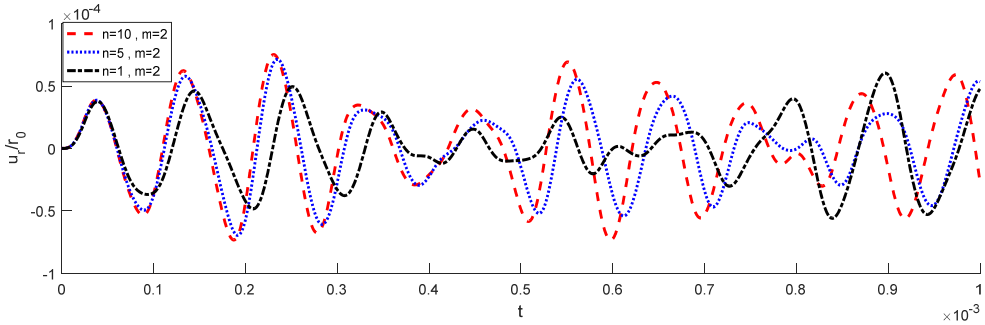

Figure 11 Radial vibrations of a cylinder with an outer radius of 0.2, an inner radius of 0.16, and a length of 0.4 for different values of *m* and *n*.

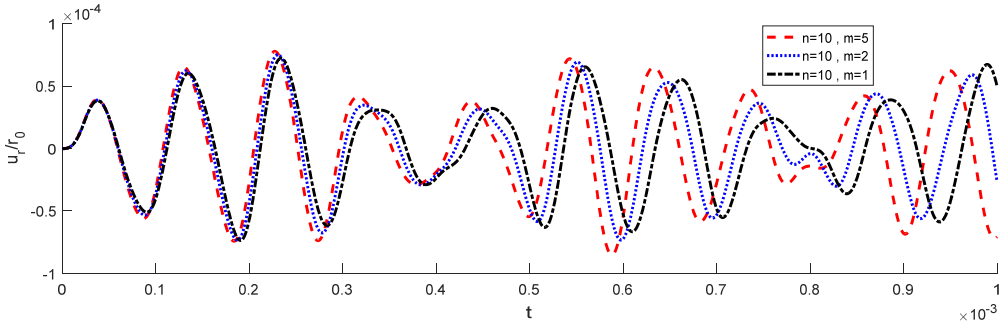

Figure 12 Radial vibrations of a cylinder with an outer radius of 0.2, an inner radius of 0.16, and a length of 0.4 for different values of *m* and *n*.

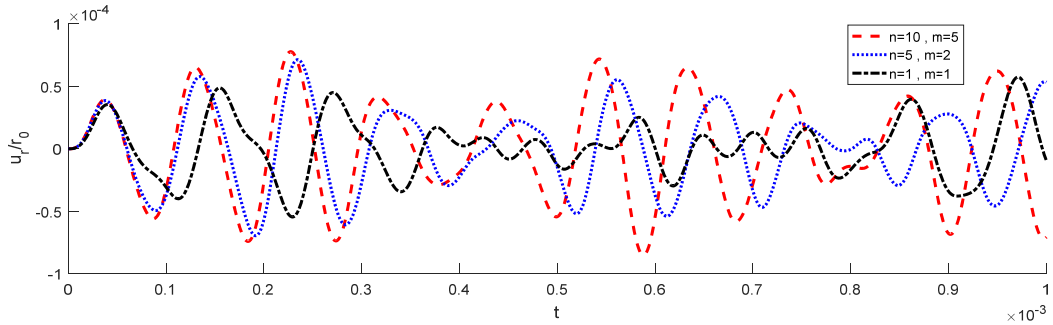

Figure 13 Radial vibrations of a cylinder with an outer radius of 0.2, an inner radius of 0.16, and a length of 0.4 for different values of *m* and *n*.

Based on the obtained figures, it is observed that an increase in the 2D-FGM cylinder thickness may either increase or decrease the radial vibrations. This highlights the fact that one can control the vibrations by changing the thickness under various conditions. As a next step, the cylinder length was shortened to 0.4 and the results were investigated again for the three cases.
Comparing Tables (3)–(5) to Figures (11)–(13), it is clear that the vibrations are attenuated upon decreasing the cylinder length.

7 Conclusion

In this paper, free and forced vibrations of cylinders made of 2D-FGM were investigated via a meshless methodology into which the MSL functions were incorporated. The FGM was assumed to be graded along both the radius and the length of the cylinder. The governing equations were established using the weak form of the equation of motion, and volumetric changes were applied to the cylinder made of FGM using power coefficients. Comparing the results of the proposed meshless method to those of the similar research works, it was concluded that the proposed methodology offered very high accuracy.
Focusing on the engineering design applications of the proposed methodology, the results of investigating the vibrations of the cylinders made of 2D-FGM confirmed that the radial vibrations could be attenuated by adjusting the power coefficients along the radius and length of the cylinder. In this case, a reduction in the power coefficient along the length of the cylinder could lower the radial vibrations. Moreover, an increase in the thickness and/or a decrease in the length of a cylinder made 2D-FGM could enhance the resultant natural frequency, and the enhancement of the natural frequency was be function of the power coefficients.

References

[1] Loy, C.T., Lam, K.Y., and Reddy, J.N., "Vibration of Functionally Graded Cylindrical Shells", International Journal of Mechanical Sciences, Vol. 41, pp. 309-324, (1999).

[2] Pradhan, S.C., Loy, C.T., Lam, K.Y., and Reddy, J.N., "Vibration Characteristics of Functionally Graded Cylindrical Shells under Various Boundary Conditions", Applied Acoustics, Vol. 61, pp. 111-129, (2000).

[3] Zhou, D., Cheung, Y. K., Lo, S. H., and Au, F. T. K., "3D Vibration Analysis of Solid and Hollow Circular Cylinders Via Chebyshev–Ritz Method", Comput. Methods Appl. Mech. Engrg. Vol. 192, pp. 1575-1589, (2003).

[4] Haddadpour, H., Mahmoudkhani, S., and Navazi, H.M., "Free Vibration Analysis of Functionally Graded Cylindrical Shells Including Thermal Effects", Thin-Walled Structures, Vol. 45, pp. 591–599, (2007).

[5] Najafizade, M.M., and Isvandzibaei, M.R., "Vibration of Functionally Graded Cylindrical Shells Based on Higher Order Shear Deformation Plate Theory with Ring Support", Acta Mech, Vol. 91, pp. 75-91, (2007).

[6] Ansari, R., and Darvizeh, M., “Prediction of Dynamic Behavior of FGM Shells under Arbitrary Boundary Conditions”, Compos. Struct. Vol. 85, pp. 284–292, (2008).

[7] Mollarazi., H. R., Foroutan, M., and Moradi-Dastjerdi, R., "Analysis of Free Vibration of Functionally Graded Material (FGM) Cylinders by a Meshless Method", Journal of Composite Materials, Vol. 46, No. 5, pp. 507-515, (2012).

[8] Foroutan, M., and Shirzadi, N., "Analysis of Free Vibration of Functionally Graded Material Cylinders by Hermitian Collocation Meshless Method", Australian Journal of Mechanical Engineering, Vol. 14, No. 2, pp. 95-103, (2016).

[9] Sadeghi Ferezghi, Y., Sohrabi, M.R., and Mosavi Nezhad, S.M., "Dynamic Analysis of Non-symmetric Functionally Graded (FG) Cylindrical Structure under Shock Loading by Radial Shape Function using Meshless Local Petrov-Galerkin (MLPG) Method with Nonlinear Grading Patterns", Computer Modeling in Engineering & Sciences, Vol. 113, No. 4, pp. 497-520, (2017).

[10] Safaeia, B., Moradi-Dastjerdib, R., Qin, Zh., and Chu, F., "Frequency-dependent Forced Vibration Analysis of Nanocomposite Sandwich Plate under Thermo-mechanical Loads", Elsevier Journal, Vol. 161, pp. 44-54, (2019).

[11] Onate, E., Idelsohn, S., Zienkiewicz, O.C., Taylor, R.L., and Sacco, C., "A Stabilized Finite Point Method for Analysis of Fluid Mechanics Problems", Comp. Methods Appl. Mech. Engen, Vol. 139, pp. 315-346, (1996).

Nomenclatures

P: Material property (e.g. Young's modulus, density, and Poisson's ratio)
P_i: Properties of the inner layers of the cylinder
P_o: Properties of the outer layers of the cylinder
V_f: Volumetric fraction of the material
m: Positive constant
n: Positive constant
σ: Vectors of stress
ε: Strain
F: Surface force
U: Displacement
Γ: Segment of the region
W: Weighting function
$a(\bar{X})$: Unknown coefficients vector
P(X): Basis vector
NP: Number of nodes within the affected region
$\Psi_I(x)$: MLS shape function
u_i : Generalized (virtual) displacement of the nodes within the affected region around the *considered point*
Ψ_i : Shape function of the i-th node
$(u_r)_i$: Components of the generalized displacement at the respective nodes**.**
$(u_z)_i$: Components of the generalized displacement at the respective nodes**.**
u_r^h : Actual displacement component along r-axis of the cylindrical coordinate system
u_z^h : Actual displacement component along z-axis of the cylindrical coordinate system